Sorbate/Sorbent Phase Transition during Adsorption of *p*-Xylene in Silicalite

S. Mohanty, H. T. Davis, A. V. McCormick
Dept. of Chemical Engineering and Materials Sciences, University of Minnesota, Minneapolis, MN 55455

An analytically solvable lattice model was used to study the difference in the physics of p-xylene adsorption in ORTHO and PARA phases of silicalite. The model predicts that a phase transition of p-xylene in the pore space does not necessarily require a silicalite-phase transition. Conditions for the sorbate-phase transition are identified. The sign of the sorbate-sorbate interactions is critical to sorbate-phase transition. It is suggested that although the sorbate- and sorbent-phase transitions can be distinct events, there is strong coupling between the two. It is reasonable to suppose that the fluid-phase change may drive the zeolite phase change. Finally, this equilibrium study suggests the possibility of hysteresis at higher coverages depending on the kinetics of adsorption.

Introduction

Adsorption of p-xylene in silicalite has been studied experimentally (Pope, 1984, 1986; Thamm, 1987a,b; Richards and Rees, 1988; Talu et al., 1989; Guo et al., 1989) and by simulations (Grauert and Fiedler, 1989; Vigne-Maeder and Jobic, 1990; Nakazaki et al., 1992; Li and Talu, 1993; Snurr et al., 1993; Mohanty et al., 1999) in part to assess whether it is possible to economically separate p-xylene (a raw material in the manufacture of terephthalic acid) from a mixture of p-, m-, and o-xylene and ethylbenzene, which is supplied by the napthacrackers or reformers (Broughton et al., 1970; Seko et al., 1979). Experiments (Fyfe et al., 1984, 1988, 1990; Reischman et al., 1988; Koningsveld et al., 1989) have shown that the sorbent phase, silicalite, undergoes a phase transition with increasing loading of p-xylene from the ORTHO phase of silicalite at a low loading to the PARA silicalite phase at a higher loading. This silicalite-phase change implies that the sorbate-sorbent interaction drives a change in the sorbent structure. This leads us to the question: can the sorbate in the pore space undergo a phase transition distinct from the sorbent phase transition? And if so, what are the conditions that drive this phase transition? In this work, we try to address these questions using principles of statistical mechanics of lattice fluids.

Lattice models have been used to study adsorption in zeolites. An analytical lattice model was developed by Lee et al. (1992) to study benzene adsorption in silicalite. However, their model predicted that the sorbate molecules will occupy the cross channel sites preferentially, which is contradictory to experimental evidence. We note that cross channels have also been referred to as sinusoidal channels and zig-zag channels in the literature. Snurr et al. (1994) used Monte-Carlo simulation based on the lattice approximation of adsorption sites to correctly predict adsorption of benzene and p-xylene in silicalite. By performing calculations for the ORTHO and the PARA silicalite structures, the model was able to account for the step in the adsorption isotherm seen in experiments. The authors attribute this feature to the ORTHO to PARA phase change in silicalite at a benzene loading of about four molecules per unit cell.

In this study, we will first present potential energy maps of p-xylene in ORTHO and PARA silicalite to get the energy of interaction of p-xylene with ORTHO silicalite and PARA silicalite (as the case may be) at the sites of adsorption and identify sorbate sites similar to the approach of Snurr et al. (1994). Using these interaction energies as parameters, we will develop an analytical lattice model to qualitatively predict adsorption behavior paying particular attention to phase transitions. We perform a similar study with m-xylene. Finally, we study adsorption of binary mixtures of p- and m-xylene in ORTHO and PARA silicalite and show that cross component sorbate-sorbate interactions influence the adsorption isotherms, as well as sorbate phase behavior.

The advantage of an approximate analytical model over Monte-Carlo simulation is that an analytical approximation can better show phase transition at different chemical potentials and temperatures; one can *know* whether there are mul-

Correspondence concerning this article should be addressed to A. V. McCormick.

tiple equilibrium solutions. The disadvantage is that, to formulate a model that is analytically tractable, one has to assume that the parameters (such as the volume and interaction energies) are independent of coverage. Further, a rigid zeolite structure is assumed. The intramolecular bonds of the sorbates are also assumed to be rigid, and no vibrational or rotational modes of freedom are considered. Universal Force Field (Rappe et al., 1992) parameters were used to represent the Lennard-Jones type potentials. Since we want to qualitatively predict the adsorption isotherm and analyze phase behavior, we feel the simplifications resulting from these assumptions justify their use.

Silicalite Pore Structure and Potential Energy Maps

ORTHO silicalite and PARA silicalite have been described by Olson et al. (1981) and Koningsveld et al. (1989). The pores in silicalite are presented in Figure 1. There are two kinds of pores: the straight channels and the cross channels that zigzag between these straight channels. The pores provide for three types of adsorption sites: those at the intersections, referred to as type 1 sites for the purpose of this study, those along the cross channels, referred to as type 2 sites, and those in the straight channels between the intersections, referred to as type 3 sites. There are four sites of each type in a unit cell. Experimental studies show that p-xylene preferentially occupies the intersections (type 1) at low loading. Then, it occupies the cross-channel sites (type 2) and silicalite undergoes a transition from the ORTHO to PARA phase. The sorbate-sorbate interaction between xylene molecules occupying adjacent type 1 and type 3 sites is strongly repulsive. (The size of the xylene molecules is large enough that steric hindrance prevents adjacent type 1-type 3 sites from being occupied. The type 1 sites being preferentially occupied, this implies that the type 3 sites will be left unoccupied.) Hence, type 3 sites are left unoccupied. Maximum coverage of such aromatic sorbates in silicalite is about eight molecules per unit cell.

Potential energy maps plot the locus of constant sorbate-sorbent interaction energy (in the sorbate's state of minimum energy with respect to rotation). These maps test whether our model predicts the sites described above and calculate the p-xylene-zeolite energy of interaction at these sites. For the calculation of potential energy maps, a unit cell of the zeolite structure was meshed by a grid (mesh size of 0.2 A was used; finer mesh sizes did not result in significantly higher accuracy, but resulted in larger storage requirements) and a single sorbate molecule was placed at a node on the grid (with the geometric center of the aromatic ring placed at the node). At any node in the zeolite grid, the sorbate was allowed three rotational degrees of freedom to find the most favorable orientation with respect to energy using a Monte-Carlo technique. Repeating such calculations throughout the zeolite grid allowed us to map the rotationally minimized potential energy for the isomers of xylene in silicalite.

In Figure 2, we show the potential energy map for a *p*-xylene inside one quadrant of a unit cell of ORTHO silicalite (by symmetry, the potential energy map in the rest of the cell can be extrapolated). The shaded region encompasses that part of the pore space that the sorbate can access easily, that is, the energy of interaction is less than +12.5 kJ/mol (approximately 5RT at 313 K). The accessible region is restricted to the channel intersections and along the axis of the straight channel. In Figure 3, we show the potential energy map for a p-xylene inside an octant of a unit cell of PARA silicalite. The accessible region lies along the straight channel and at the intersections. Sites are accessible in the cross channel too. On the other hand, m-xylene feels a repulsive

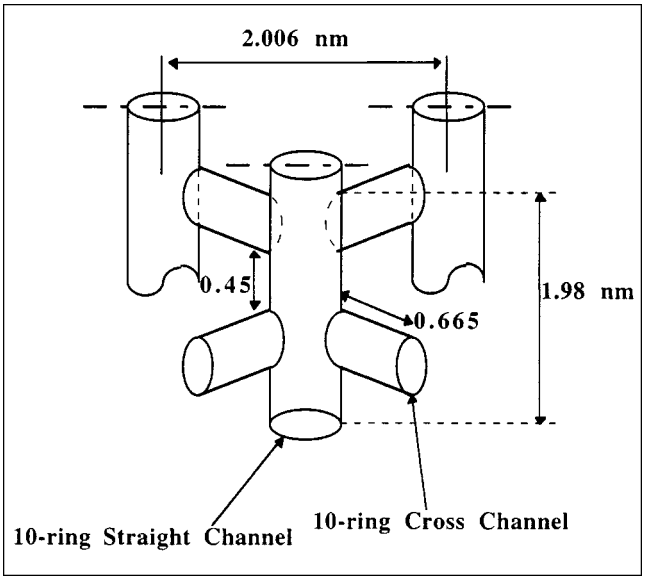

Figure 1. Pore structure of silicalite.

Dimensions are marked in nm; 1.98 nm and 2.006 nm being the dimensions of the unit cell in those directions.

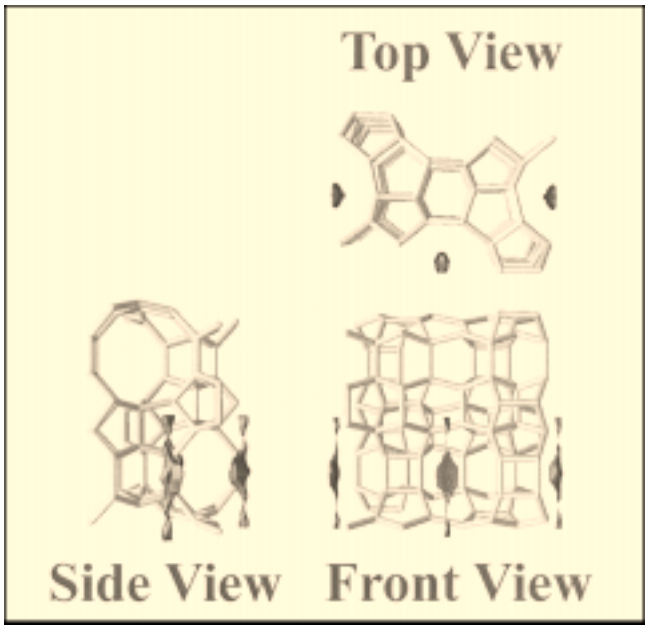

Figure 2. Orthographic view of a constant potential energy surface of *p*-xylene in the ORTHO phase of silicalite at 12.5 kJ/mol.

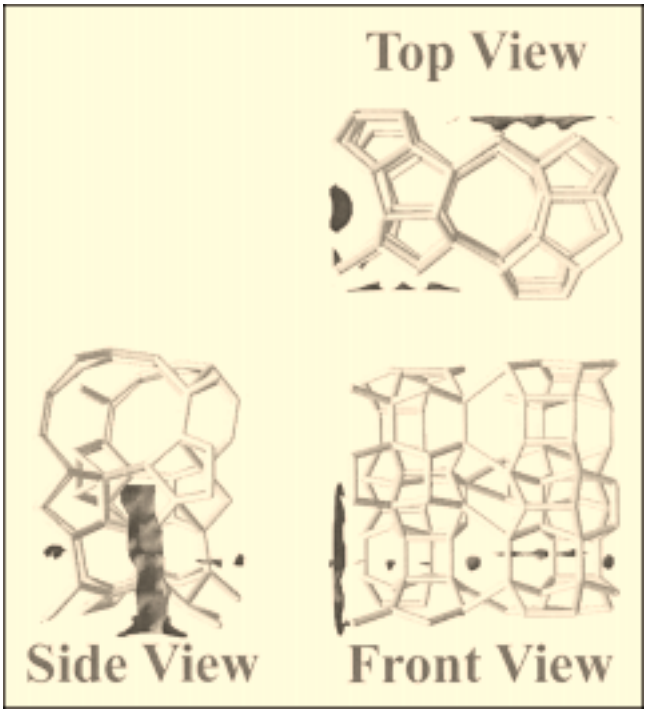

Figure 3. Orthographic view of a constant potential energy surface of *p*-xylene in the PARA phase of silicalite at 12.5 kJ/mol.

energy of interaction greater than 12.5 kJ/mol throughout the pore space of ORTHO silicalite. This suggests that it will not adsorb in ORTHO silicalite. In PARA silicalite, however, m-xylene is able to access the intersections and parts of the cross channels, as evident from Figure 4—the potential energy map of m-xylene in PARA silicalite at 12.5 kJ/mol.

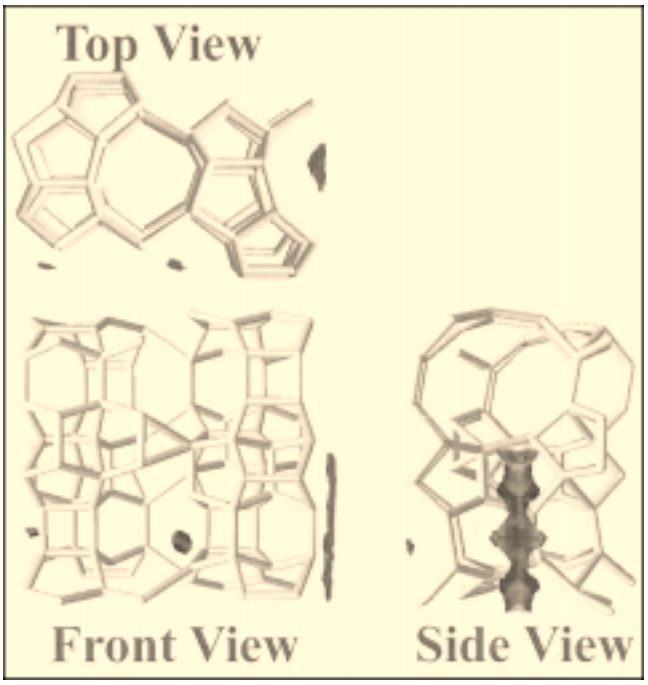

Figure 4. Orthographic view of a constant potential energy surface of *m*-xylene in the PARA phase of silicalite at 12.5 kJ/mol.

Lattice Model for Single Component Adsorption

We will use an analytical lattice model assuming only nearest neighbor interactions to predict the adsorption isotherm and compare it to experimental data. For a canonical ensemble with coverage of N p-xylene molecules per unit cell (for N_1 adsorbates in M_1 sites of type 1 and N_2 adsorbates in M_2 sites of type 2) at a temperature T, the canonical partition function $Q(N_1\ N_2\ M_1\ M_2\ T)$ can be expressed as

$$Q(N_1 N_2 M_1 M_2 T) = \frac{M_1!}{N_1!(M_1 - N_1)!}\frac{M_2!}{N_2!(M_2 - N_2)!} q_1^{N_1} q_2^{N_2} e^{-V/kT} \quad (1)$$

where q_1 and q_2 are the site partition function for sites of each type and V is the potential energy at this loading, with contributions from sorbate-sorbate, as well as from sorbate-sorbent interactions. The site partition function is

$$q_i = \left(\frac{\nu_i}{\Lambda^3}\right) \quad (2)$$

where subscript i represents the site type, ν_i is the volume of the site—the region of the pore that can be accessed by the sorbate. In general the effective volume of the site is dependent on temperature and coverage since the lattice is affected by temperature, as well as by the presence of other guest molecules. However, we will neglect lattice relaxation and, hence, assume volume to be constant with N and T. We can estimate the volume of the sites from the potential energy maps by calculating the ratio of points in the region of the site with energy less than a cut-off energy (for example, 5 times RT, where R is the Universal Gas Constant; this encompasses 99% of the accessible volume) to the total number of points in the unit cell multiplied by the volume of the unit cell. Λ is the thermal deBroglie wavelength defined as

$$\Lambda = \frac{h}{\sqrt{2\pi mkT}} \quad (3)$$

where h is the Planck's constant, k is the Boltzmann constant, and m is the mass of the sorbate molecule. We neglect any vibrational degrees of freedom.

Next, we need to determine the values of the energies of interaction between two sorbates and between the sorbate and the lattice. The sorption sites are so located in the sorbent that we can neglect all three body interactions. In the real system, the energies of interaction will vary within a site. Hence, we have to define some sort of average energy of interaction (averaged over the site volume as defined earlier). The energies in the appropriate configuration partition function occur as contributions to the exponent of the net poten-

tial energy. Thus, we will define an sorbate-sorbent free energy as

$$\exp\left(-\frac{\langle \epsilon_{la_j}\rangle}{RT}\right)\int_j d^3r_{a_j} = \int_j d^3r_{a_j} \times \exp\left(-\frac{u_{la_j}(r_{a_j})}{RT}\right) \quad (4a)$$

where subscript j refers to the type of site. $\langle \epsilon \rangle$ is the free energy of the sorbate at the site and includes translational and rotational degrees of freedom, with subscript la_j referring to the sorbent lattice-adsorbate interaction at site j. u_{laj} is the energy of interaction between a sorbate (located at r_{aj} in the site) and the sorbent lattice. A Monte-Carlo method is used to evaluate the integral. The sorbate molecule is allowed to freely rotate and translate within the pore space. The integrals are over the space where the p-xylene-zeolite energy of interaction is less than $+5$RT. The integral on the lefthand side, thus, is the volume of the site as defined earlier. Similarly, we will define the sorbate-sorbate free energy as

$$\exp\left(-\frac{\langle \epsilon_{a_ia_j}\rangle}{RT}\right)\int_i d^3r_{a_i}\int_j d^3r_{a_i} = \iint_{i,j} d^3r_{a_i} d^3r_{a_j} \times \exp\left(-\frac{u_{a_ia_j}(r_{a_i}, r_{a_j})}{RT}\right) \quad (4b)$$

$u_{a_ja_j}$ is the energy of interaction between a sorbate located at position r_{ai} in site i and another sorbate located at position r_{aj} in an adjacent site j. The integrals are over the sites i and j. Again, a Monte Carlo technique is used to evaluate the integrals. Both molecules are allowed to translate and rotate independently. Only those positions are included in the integral that have a value of u_{laj} less than $+5$RT. The integral is evaluated for values of $u_{a_ia_j}$ less than $+5$RT (configurations with $u_{a_ia_j}$ greater than $+5$RT will contribute negligibly to the integral). The values of the interaction energies of p-xylene in ORTHO silicalite and PARA silicalite, as well as the sorbate-sorbate interactions (as calculated from Eqs. 4a and 4b) are listed in Table 1. The p-xylene-zeolite interaction energies at the intersections for the ORTHO and PARA phases compare well with the calculations of Snurr et al. (1993). Unlike Snurr et al. (1993)—who notice no adsorption in the cross channel sites despite an attractive interaction energy—in the ORTHO phase we observe no attractive interaction with p-xylene in the cross channel.

Under the approximation of only nearest neighbor interactions, a mean field approximation of the potential energy V can thus be expressed as

$$V = N_1\epsilon_{la_1} + N_2\epsilon_{la_2} + \epsilon_{a_1a_2}\frac{N_1^2 z_1}{2M_1} + \epsilon_{a_2a_2}\frac{N_2^2 z_2}{2M_2} + \frac{1}{2}\left[\epsilon_{a_1a_2}\frac{N_1N_2z_{12}}{M_2} + \epsilon_{a_1a_2}\frac{N_1N_2z_{21}}{M_1}\right] \quad (5)$$

A type 1 site has 2 nearest neighbors of type 1 (denoted by coordination number $z_1 = 2$) and 2 of type 2 ($z_{12} = 2$). Sites of type 2 have no nearest neighbors of type 2 ($z_2 = 0$) and 2 of type 1 ($z_{21} = 2$). The first two terms on the righthand side represent the sorbate-sorbent interaction, and all the other term account for sorbate-sorbate interactions—the third term takes interactions between type 1 sites, the fourth term is zero since z_2 is zero, and the fifth and sixth terms represent interactions between sorbates at sites of type 1 and 2. The factor of half avoids counting interactions twice. $\epsilon_{a_ia_j}$ is the sorbate-sorbate interaction between sorbate occupying sites of type i and j. ϵ_{lai} is the potential energy of interaction between the adsorbate and the zeolite.

Approximate methods have to be used in treatment of a two- or three-dimensional lattice statistics problem incorporating interacting sites. For this work, we will use Bragg-Williams approximation (Hill, 1986). As per this approximation for a lattice model with nearest neighbor interactions, the configuration degeneracy and average nearest neighbor interaction energy are both calculated on the basis of a random distribution of molecules among sites. In this particular case though, the distribution is not completely random. Whether an intersection or cross-channel site is chosen is dependent on the interaction energies, as will be clear in a later section. However, the location of the intersection or cross-channel site (once chosen) is random. Thus, this approximation will not take account of short-range clustering, although long-range phase behavior can be accounted for. Other implications of this approximation will be detailed in the end of this work.

The grand canonical potential Ω for such a lattice equilibrated with an external fluid at a chemical potential μ is

$$\Omega = U - TS - \mu N \quad (6)$$

where the internal energy U and entropy S can be evaluated as

$$U = kT^2\left(\frac{\partial \ln Q}{\partial T}\right)_{M_i, N_i} \quad (7)$$

and

$$S = k\ln Q + kT\left(\frac{\partial \ln Q}{\partial T}\right)_{M_i, N_i} \quad (8)$$

Using Eq. 1

$$U = 3NkT + V \quad (9)$$

Table 1. Parameters for the Lattice Model for p-xylene Adsorbing in ORTHO and PARA Silicalite from Atomistic Calculations

	ORTHO Silicalite (303 K)	PARA Silicalite (303 K)
υ_1	23.91 A^3	78.73 A^3
υ_2	0.26 A^3	0.31 A^3
ϵ_{la1}	-55 kJ/mol	-45 kJ/mol
ϵ_{la2}	60 kJ/mol	-60 kJ/mol
ϵ_{a1a1}	-1 kJ/mol	-1 kJ/mol
ϵ_{a1a2}	-20 kJ/mol	-20 kJ/mol

$$S = 3Nk + k\ln\left[\frac{M_1!}{N_1!(M_1-N_1)!}\frac{M_2!}{N_2!(M_2-N_2)!}\right] + k\ln\left[\frac{\nu_1^{N_1}\nu_2^{N_2}}{\Lambda^{3N}}\right] \quad (10)$$

Applying Stirlings approximation to the grand canonical potential

$$\Omega = V + kTN\ln(\Lambda^3) - kT \times \begin{Bmatrix} N_1\ln(\nu_1) + M_1\ln M_1 - N_1\ln N_1 \\ -(M_1-N_1)\ln(M_1-N_1) + N_2\ln(\nu_2) + M_2\ln M_2 \\ -N_2\ln N_2 - (M_2-N_2)\ln(M_2-N_2) \end{Bmatrix} - N\mu \quad (11)$$

The numerical prefactor in the first term of Eqs. 9 and 10 accounts for the degrees of freedom of the sorbate molecules. They are influenced by the assumptions we make, in this case that only translational and rotational modes are operable. In any case, these terms cancel out in Eq. 11.

The adsorption isotherm can now be obtained by minimizing the grand canonical potential with respect to the total number of sorbate molecules. Derivation of the adsorption isotherm of p-xylene in ORTHO and PARA silicalite with changing temperature and chemical potential (pressure) will be presented separately in subsequent sections.

Adsorption of p-Xylene in Silicalite

Adsorption in ORTHO silicalite

In this part of the work we obtain the adsorption isotherm (that is, N as a function of μ and T) for p-xylene in ORTHO silicalite from Eq. 11 and analyze the significance of the various energy parameters on adsorption. To do so, however, we need to derive a relationship between N_1 (coverage at type 1 sites) and N (total coverage). By minimizing Ω (and changing from a molecular to a molar basis), we can calculate the fraction of sorbate molecules adsorbed in type 1 sites at equilibrium. (Note that $dN_1 = -dN_2$.) Performing the operation, we find

$$\left(\frac{\partial\Omega}{\partial N_2}\right)_{N,T} = \left(\frac{\partial V}{\partial N_2}\right)_{N,T} - RT\left\{\ln\frac{\nu_2}{\nu_1} - \ln\frac{(M_1-N_1)}{N_1} + \ln\frac{(M_2-N_2)}{N_2}\right\} = 0 \quad (12)$$

where

$$\left(\frac{\partial V}{\partial N_2}\right)_{N,T} = -\epsilon_{la_1} + \epsilon_{la_2} - \frac{\epsilon_{a_1a_1}z_1N_1}{M_1} + \frac{1}{2}\epsilon_{a_1a_2}(N_1-N_2)\left\{\frac{z_{12}}{M_2} + \frac{z_{21}}{M_1}\right\} \quad (13)$$

The criterion for a minimum free energy is, thus,

$$0 = -\epsilon_{la_1} + \epsilon_{la_2} - \frac{\epsilon_{a_1a_1}N_1}{2} + \frac{1}{2}\epsilon_{a_1a_2}(N_1-N_2) - RT\left\{\ln\left(\frac{4/N_2-1}{4/N_1-1}\right) + \ln\left(\frac{\nu_2}{\nu_1}\right)\right\} \quad (14)$$

For p-xylene adsorbing in ORTHO silicalite, the interaction energy parameters are listed in Table 1. The sorbate-sorbate interactions between sites of type 1 ($\epsilon_{a1a1} \approx -1$ kJ/mol) is much smaller than between sites of type 1 and type 2 ($\epsilon_{a1a2} \approx -20$ kJ/mol) and, therefore will be neglected. Let us consider a system with a total of four molecules per unit cell, that is, the sum of N_1 and N_2 is 4 ($= N$). Equation 14 can then be rewritten as

$$RT\ln\left(\frac{\nu_1}{\nu_2}\right) + \frac{1}{2}\epsilon_{a_1a_2}(4-2N_2) + 2RT\ln\left(\frac{N_2}{4-N_2}\right) = -(\epsilon_{la_2} - \epsilon_{la_1}) \quad (15)$$

Solving for N_2, we find that

$$N_2 \approx \frac{4}{1+\sqrt{\frac{\nu_1}{\nu_2}}\,e^{\{\epsilon_{la2}-\epsilon_{la1}+2\epsilon_{a1a2}\}/2RT}} \quad (16)$$

where we have anticipated that $N_2 \ll 1$.

In the temperature range of 273 to 350 K (this is the temperature range of experiments in literature), we find that N_2 is about 10^{-5}. There is little occupancy in the type 2 sites until the type 1 sites are occupied at a coverage of 4 molecules per unit cell. Thus, this lattice model agrees with observations from NMR data and crystallographic studies (Fyfe et al., 1984, 1988, 1990; Reischman et al., 1988; Koningsveld et al., 1989). Thus, we have a relationship

$$N_1 \approx \begin{Bmatrix} N : \forall N < 4 \\ 4 : \forall N > 4 \end{Bmatrix}; \quad N_2 = N - N_1 \quad (17)$$

Substituting Eq. 17 in Eq. 11, for $N < 4$

$$\Omega = V + kTN_1\ln(\Lambda^3) - kT\{N_1\ln(\nu_1) + M_1\ln M_1 - N_1\ln N_1 - (M_1-N_1)\ln(M_1+N_1)\} - N_1\mu \quad (18)$$

where the coverage N_1 is less than or equal to four molecules per unit cell and V—the potential energy—now accounts only for interaction with type 1 sites and is expressed as

$$V = N_1\epsilon_{la_1} + \epsilon_{a_1a_1}\frac{N_1^2z_1}{2M_1} \quad (19)$$

The partial derivative of Ω with respect to N_1 at constant T, v, μ can be expressed as

$$\left(\frac{\partial\Omega}{\partial N_1}\right)_{\mu,T} = 0 = \left(\frac{\partial V}{\partial N_1}\right)_{\mu,T} + kT\{\ln\Lambda^3 - \ln\nu_1 + \ln N_1 - \ln(M_1-N_1)\} - \mu \quad (20)$$

where

$$\left(\frac{\partial V}{\partial N_1}\right)_{\mu,T} = \epsilon_{la_1} + \frac{N_1 z_1 \epsilon_{a_1 a_1}}{M_1} \tag{21}$$

The second term in Eq. 21 is much smaller than the first and will be neglected. Equations 20 and 21 yield the result

$$N_1 = \frac{M_1}{1 + \frac{\Lambda^3}{\nu_1} e^{-((\mu - \epsilon_{la_1})/RT)}};$$

$$N < 4;$$

$$N_2 \approx 0 \tag{22}$$

Using Eq. 17 for $N > 4$, the grand canonical potential is minimized again with respect to N_2 to obtain the adsorption isotherm under the given conditions

$$\left(\frac{\partial \Omega}{\partial N_2}\right)_{N,T} = 0 = \left(\frac{\partial V}{\partial N_2}\right)_{N,T} - \mu - kT\left\{\ln \nu_2 - \ln N_2 + \ln(M_2 - N_2) - \ln(\Lambda^3)\right\} \tag{23}$$

where

$$\left(\frac{\partial V}{\partial N_2}\right)_{N,T} = \epsilon_{la_2} + \frac{1}{2}\epsilon_{a_1 a_2} N_1 \left\{\frac{z_{12}}{M_2} + \frac{z_{21}}{M_1}\right\} \tag{24}$$

Solving Eqs. 23 and 24 for N_2

$$N_2 = \frac{M_2}{1 + \frac{\Lambda^3}{\nu_2} e^{-((\mu - \epsilon_{la_2} - 2\epsilon_{a_1 a_2})/RT)}};$$

$$N > 4;$$

$$N_1 = N - N_2 \tag{25}$$

The total coverage N is the sum of Eqs. 22 and 25 which is

$$N = \frac{M_1}{1 + \frac{\Lambda^3}{\nu_1} e^{-((\mu - \epsilon_{la_1})/RT)}}; N < 4;\ \mu \le \mu_C$$

$$N = 4 + \frac{M_2}{1 + \frac{\Lambda^3}{\nu_2} e^{-((\mu - \epsilon_{la_2} - 2\epsilon_{a_1 a_2})/RT)}}; N > 4;\ \mu > \mu_C \tag{26}$$

μ_c is the smallest value of the chemical potential at which N equals 4. The first expression for N will be used for values of chemical potential less than μ_c. Subsequently, the second expression for N should be used.

The second-order virial equation of state for p-xylene with the Pitzer-Curl-Tsonopoulos correlation (Prausnitz et al. (1986) suggests that this correlation is a reasonable approximation for this class of compounds up to moderate atmospheres-say 5 bars) is used to convert the chemical potential to pressure at the given temperature. Figure 5 shows pressure as a function of chemical potential for p- and m-xylene at a few temperatures spanning the temperature range (273k–350K) in which experiments have been performed.

In Figure 6, we present the adsorption isotherm based on the prediction of Eq. 26 with increasing temperature. The shape of the isotherms are similar to those presented by Talu et al. (1989) at low coverage. There is an initial increase in adsorption with increasing pressure. Subsequently, the isotherms plateau at four molecules per unit cell, when all the intersection sites are occupied. This is in agreement with the simulations of Snurr et al. (1993). We see no adsorption in the cross-channel sites at any of the temperatures and pressures explored. With decreasing temperature, we observe that adsorption becomes increasingly easier and saturation is achieved more at lower pressures. However, the predicted effect of temperature is not as significant as observed in the experimental data of Talu et al. (1989). We notice that the adsorption isotherms have the form of the Langmuir isotherm. This is true for this specific case of p-xylene in ORTHO sili-

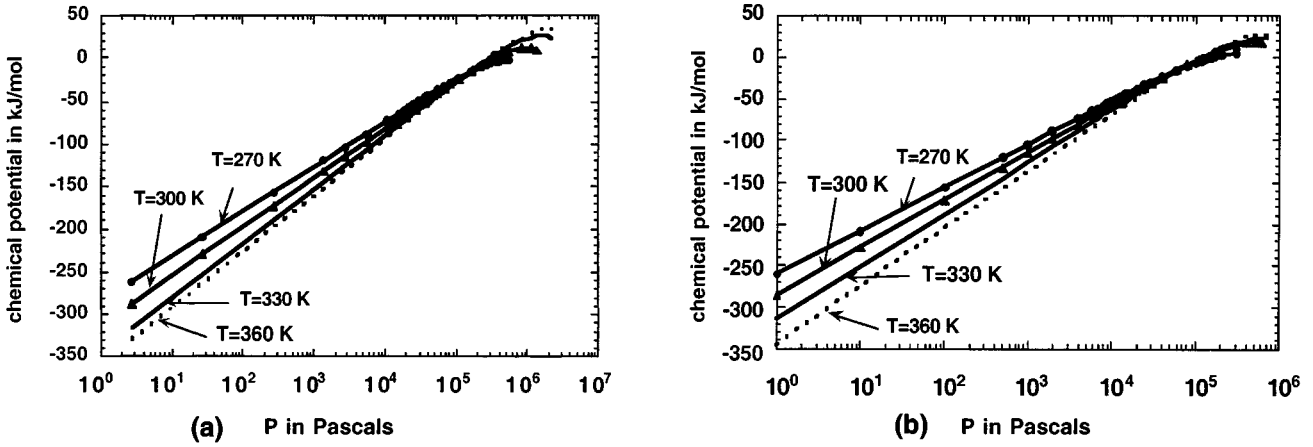

Figure 5. Pressure as a function of chemical potential and temperature using second-order Virial equation of state (a) for *p*-xylene and (b) for *m*-xylene.

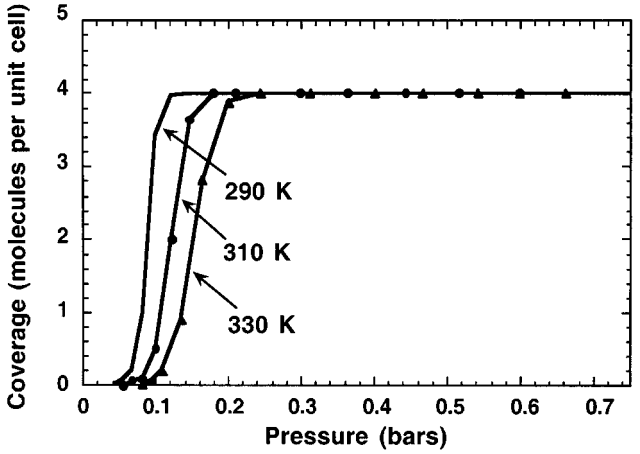

Figure 6. Lattice model predictions of the adsorption isotherms of *p*-xylene in ORTHO silicalite.

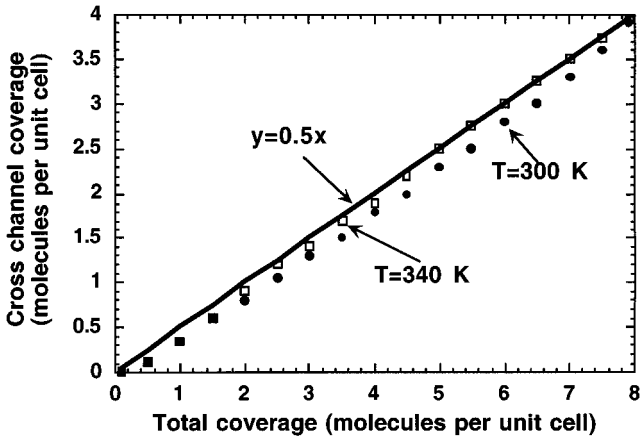

Figure 8. Occupancy of cross-channel sites relative to total occupancy of *p*-xylene in PARA silicalite.

calite. At low loadings (< 4 molecules per unit cell), there is no nearest neighbor interaction. Thus, the system can be modeled by a Langmuir model. However, in the case of p-xylene in PARA silicalite, nearest neighbor interactions will become important and we will see that the Langmuir-like model will not be adequate. The Langmuir-like model will also fail at low temperatures for p-xylene in ORTHO silicalite.

Equation 26 does not have multiple roots. Thus, this model suggests an absence of a two-phase region at this stage of adsorption. However, if the temperature is low enough (< 100 K), the sorbate-sorbate interaction term in Eqs. 20 and 21 cannot be neglected. Under these circumstances, the system will have multiple roots and then phase transition is possible. By analyzing Eqs. 20 and 21, we can estimate the conditions of temperature and pressure (or chemical potential) when multiple equilibrium states will be possible. The domain of conditions for existence of multiple roots (multiple phases) is plotted in Figure 7 and is enclosed within the curve. From the figure, we can estimate that an upper critical temperature exists at about 40 K. Our operating conditions are well above that temperature.

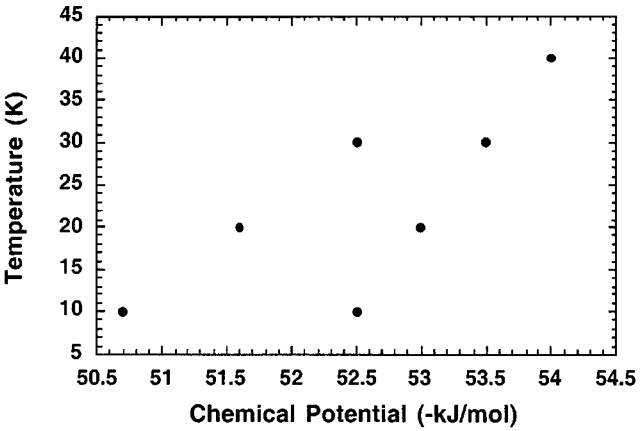

Figure 7. Two-phase domain of *p*-xylene in ORTHO silicalite.

Adsorption in PARA silicalite

For p-xylene adsorbing in PARA silicalite, we go through the same analysis as was performed for ORTHO to obtain Eq. 14. The energy parameters are listed in Table 1. ϵ_{a1a1} is much smaller than e_{a1a2} and will be neglected. To find the fraction of type 2 sites occupied when N molecules have adsorbed into a unit cell of silicalite, we replace N_1 by $N - N_2$ in Eq. 14 and solve for N_2 at various values of N and at different temperatures. Figure 8 shows the number of cross-channel sites occupied at various degrees of total coverage at 300 K and 340 K. These points are compared with a line ($N_2 = 0.5$ N) representing a state where half of the total coverage would be in the cross-channel sites. The plot shows that the simulation results are rather close to this line. Thus, this model concurs with the results of Snurr et al. (1993) that both intersections and cross-channel sites in PARA silicalite fill up with equal ease. For the rest of this study, we will assume that in the case of PARA, $N_2 = N_1$.

Assuming that $N_2 = N_1$, we can differentiate Eq. 11 to obtain

$$0 = \frac{\epsilon_{la_1} + \epsilon_{la_2}}{2} + \frac{N}{8}(\epsilon_{a_1a_1} + \epsilon_{a_1a_2}) + RT \ln\left(\frac{\Lambda^3}{\sqrt{\nu_1\nu_2}}\right) - \mu - RT \ln\left(\frac{2M}{N} - 1\right) \quad (27)$$

where $M \sim M_1 \sim M_2$. N can be obtained as the root of this equation. At very low chemical potentials, Eq. 27 has only one root ($N \approx 0$) representing the zero coverage limit. Equation 27 has three roots for chemical potential in the range -130 to -80 kJ/mol. Figure 9 gives an example of these roots at 303 K under the constraint of a fixed zeolite lattice. The straight line consists of the first four terms in Eq. 27. The curve represents the logarithmic term. This analysis thus proves that the model predicts the existence of a two-phase

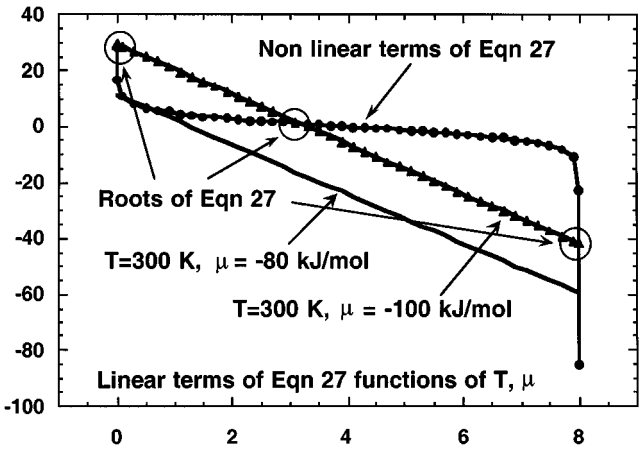

Figure 9. Sample calculation of the multiple roots to determine the two-phase domain of *p*-xylene in PARA silicalite.

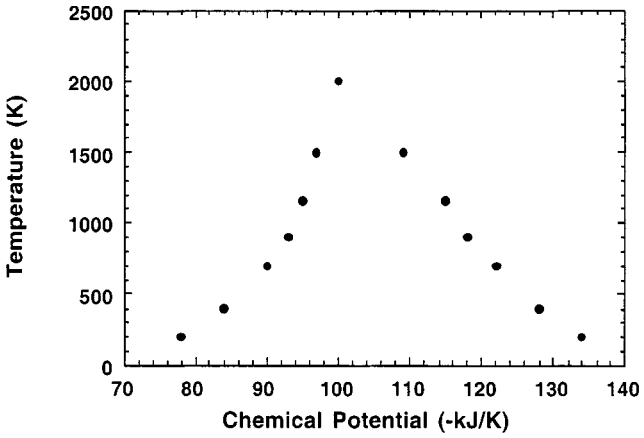

Figure 11. The two-phase domain of *p*-xylene in PARA silicalite.

region in the sorbate fluid. At higher chemical potentials (> −80 kJ/mol), there is only one root at close to eight molecules per unit cell representing the maximum coverage limit. Figure 10 shows the adsorption isotherms obtained from the roots of Eq. 27 at 303 and 333 K. Saturation is achieved at a coverage of about eight molecules per unit cell. Unlike adsorption in the ORTHO phase, we do not see any intermediate saturation. Adsorption becomes progressively more difficult with increasing temperature.

An issue that needs to be addressed is what causes the existence of multiple equilibrium states. Considering Figure 9, we notice that multiple roots are possible only if the slope of the straight line is negative *and* the intercept is in a certain range. The slope is defined by the sorbate-sorbate interactions. Repulsive sorbate interactions cannot drive a phase transition. Further, constraint on the intercept implies that the driving force—the chemical potential—should have an intermediate value. The exact range will be governed by the sorbate-pore interactions—the energetic contributions—and the volume of the sites—the entropic contributions. If the driving force is too high, coverage is close to saturation; if it is too low, sites are almost empty. In either case phase transition does not occur. Further analysis of Eq. 27 will help specify the conditions of temperature and pressure (chemical potential) where multiple roots (two-phase region) exist. These conditions are shown in Figure 11. The upper critical temperature is about 2,000 K. This is well above the operating temperature. Thus, we see that, under the conditions of interest, the sorbate in PARA silicalite will have two stable states and one unstable state. This leads to the question of which state is the system likely to be in and under what conditions do transitions between these states occur. The answer to this question will have to account for kinetics of adsorption and the details of the ORTHO silicalite-PARA silicalite coexistence curve. Thus, we see suggestions of hysteresis on the adsorption isotherm. Richards and Rees (1988) observed hysteresis in their isotherms, and Pope (1984, 1986) reported no hysteresis while Talu et al. did not comment on the issue. Based on the equilibrium states of this study, we can conclude that hysteresis is a possibility.

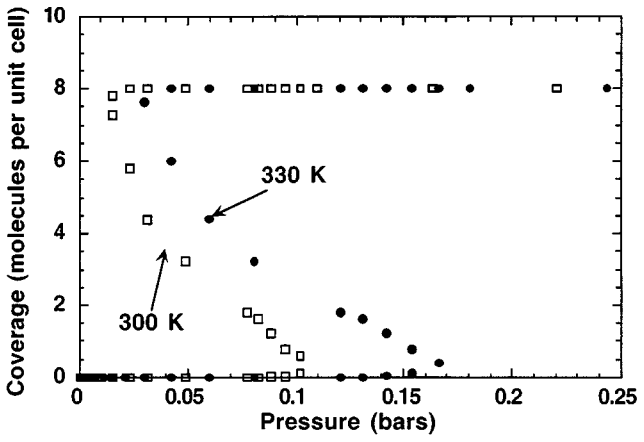

Figure 10. Lattice model predictions of the adsorption isotherms of *p*-xylene in PARA silicalite.

Comparison of Adsorption in PARA and ORTHO

Snurr et al. (1993) predicted the adsorption isotherm as a result of a change in the silicalite phase by merging the low coverage results from ORTHO with the high coverage results from PARA. In Figure 12, we compare the adsorption isotherms from ORTHO and PARA with experimental data from Richards and Rees (1988) at 310 K. At low pressures, we assume that the ORTHO phase results predict the experimental data. With an increase in coverage, we should shift to the PARA results in a manner suggested by Snurr et al. (1993). We must remember, though, that the relative positions of the isotherms in ORTHO and PARA might shift as a result of our assumptions of rigid lattice, neglect of partial charges, and choice of equation of state used to convert chemical potential to pressure. This accounts for some of the difference between the predicted and experimental results.

To identify the adsorption isotherm across the sorbent-phase transition, we have to know the conditions (of pressure, or chemical potential) at which a transition occurs from

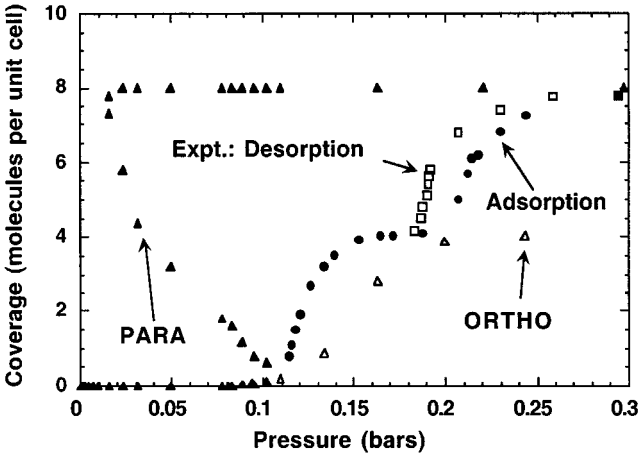

Figure 12. Comparison of adsorption isotherms predicted for *p*-xylene in PARA and ORTHO silicalite with experimental results of Richards and Rees (1988).

the stable solution in ORTHO silicalite to PARA silicalite. The situation is further complicated by the observations of Koningsveld et al. (1989) that, at coverages between four to six p-xylene molecules per unit cell, mixtures of ORTHO and PARA silicalite have been observed. This is reflected in the curvature of the adsorption isotherm between four and eight molecules per unit cell. A phase transition of the complete crystal at four molecules per unit cell would suggest a step change in the adsorption isotherm. This suggests the possibility of phase coexistence. In the absence of silicalite-phase diagrams and measurements of energy of the silicalite-phase transition, we cannot identify the conditions where a transition in the adsorption isotherm will occur.

Another question that needs to be answered now concerns how the sorbent and sorbate phase transitions affect each other. Any extensive validation of these will need more rigorous analysis. However, some comments based on literature and from this study can be made. From the work of Koningsveld et al. (1989), we know that the sorbent-phase change is driven by adsorption. In this study we found that sorbate-phase change can occur without the sorbent-phase change. In that sense, it is a distinct phenomenon. However, we do not see the strong influence of temperature on sorption observed by Talu et al. (1989) when we assume a rigid lattice that precludes phase change of the sorbent. Thus, we think the sorbent-phase change influences the sorbate-phase change. Simulation studies of p-xylene adsorbing in rigid ORTHO and PARA silicalite (Mohanty et al., 2000), on the other hand, suggest that the sorbent-phase transition might be driven by the entropy of the p-xylene sorbate. The sorbate and the sorbent-phase change occur at about a coverage of four molecules per unit cell. These facts reinforce our opinion that the two-phase transitions are strongly coupled.

Adsorption of m-Xylene in Silicalite

For comparison purposes, adsorption of m-xylene in silicalite is presented here. Table 2 shows the parameters for

Table 2. Parameters for the Lattice Model for m-xylene Adsorbing in ORTHO and PARA Silicalite from Atomistic Calculations

	ORTHO Silicalite (303 K)	PARA Silicalite (303 K)
v_1	—	42.37 A^3
v_2	—	0.28 A^3
ϵ_{la1}	70 kJ/mol*	−1.7 kJ/mol
ϵ_{la2}	2,000 kJ/mol*	1.5 kJ/mol
ϵ_{alal}	−1 kJ/mol	−1 kJ/mol
ϵ_{a1a2}	−8 kJ/mol	−8 kJ/mol

*Since there is no region in the pores where m-xylene has an energy of interaction less than +12.5 kJ/mol, the values listed here are the local minima.

m-xylene in ORTHO and PARA phases of silicalite. Clearly, *m*-xylene will not adsorb in the ORTHO phase at any reasonable pressure. Our calculations based on the lattice model for ORTHO, shows that there is no adsorption up to five atmospheres pressure. For *m*-xylene adsorbing in PARA silicalite, we perform an analysis similar to *p*-xylene in PARA silicalite. The number of cross-channel sites occupied per unit cell at various degrees of loading are shown in Figure 13. The intersections are occupied more easily than the cross channel sites. From Eq. 14 and Table 2, we obtain

$$\frac{dN_2}{dN} = \frac{3.5 - \dfrac{4RT}{(N - N_2)(4 - N + N_2)}}{7.5 + \dfrac{4RT}{N_2(4 - N_2)} - \dfrac{4RT}{(N - N_2)(4 - N + N_2)}} \quad (28)$$

Using Eq. 28 to minimize Eq. 14, we can generate the adsorption isotherm. At a pressure of 5 atm at 270 K, as little as 0.002 molecules of *m*-xylene adsorb in a unit cell of PARA silicalite. This is in agreement with simulation results in an earlier work (Mohanty et al., 2000). From Figure 13, we know that, all the adsorbed m-xylene at that coverage would occupy the intersections.

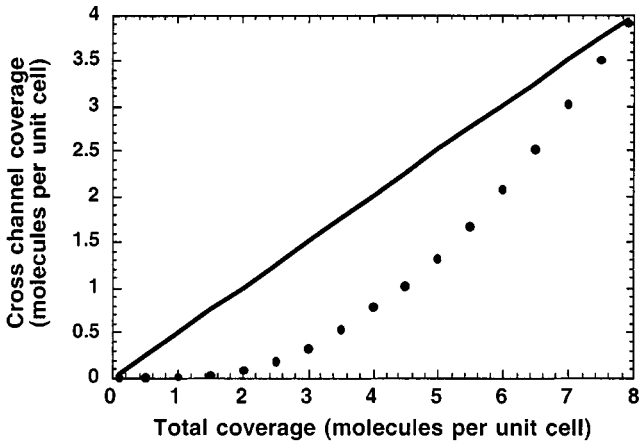

Figure 13. Occupancy of cross-channel sites by *m*-xylene in PARA silicalite relative to total occupancy.

Adsorption of Xylene Mixture in Silicalite

Lattice model

Having analyzed single component adsorption, we now turn our attention to adsorption of mixtures. The canonical ensemble for the adsorption of a binary mixture of p- and m-xylene in silicalite at temperature T can be described as

$$Q(N_{ip}, N_{2p}, N_{1m}, N_{2m}, M_1, M_2, T) = \frac{M_1!}{N_{1p}!N_{1m}!(M_1 - N_{1m} - N_{1p})!} \frac{M_2!}{N_{2p}!N_{2m}!(M_2 - N_{2p} - N_{2p} - N_{2m})!}\Theta \quad (29)$$

where N_{1p} and N_{2p} are the number of p-xylene molecules per unit cell adsorbed in sites 1 and 2, respectively; N_{1m} and N_{2m} are the number of m-xylene molecules per unit cell adsorbed in sites 1 and 2, respectively

$$\Theta = q_{1m}^{N1m} q_{2m}^{N2m} q_{1p}^{N1p} q_{2p}^{N2p} e^{-V/KT} \quad (30)$$

where q_i is the site partition function defined in Eq. 2. For the case of binary mixtures, the potential energy, V, defined as a mean field approximation, includes contributions from sorbate-sorbate interactions between the two components occupying different sites

$$V = V_{pz} + V_{mz} + V_{pp} + V_{mm} + V_{pm} \quad (31)$$

where V is the sum of the p-xylene-silicalite interaction, the m-xylene-silicalite interaction, p-xylene-p-xylene interaction, m-xylene-m-xylene interaction, and m-xylene-p-xylene interaction in that order. These are described as follows

$$V_{pz} = N_{p1}\epsilon_{p1} + N_{p2}\epsilon_{p2} \quad (32)$$

$$V_{pp} = \epsilon_{p1p1}\frac{N_{1p}^2 z_1}{2M_1} + \epsilon_{p2p2}\frac{N_{2p}^2 z_2}{2M_2} + \epsilon_{p1p2}\frac{N_{1p}N_{2p}z_{12}}{M_2} \quad (33)$$

$$V_{pm} = \epsilon_{p1m1}\frac{N_{1m}N_{1p}z_1}{2M_1} + \epsilon_{p2m2}\frac{N_{2m}N_{2p}z_2}{2M_2} + \epsilon_{m1p2}\frac{N_{1m}N_{2p}z_{12}}{M_2} + \epsilon_{m2p1}\frac{N_{2m}N_{1p}z_{12}}{M_2} \quad (34)$$

Equations for V_{mz} and V_{mm} can be expressed similarly to Eqs. 32 and 33. The subscripts m and p refer to m- and p-xylene. (Comparing with the notation in the earlier part of this work, we have dropped the subscript a referring to the adsorbate.) The interaction energies averaged over the adsorption sites are of the form described by Eqs. 4a and 4b. The Gibbs free energy G can be obtained as

$$G = V + kT\begin{bmatrix} N\ln\Lambda^3 - N_{1p}\ln\nu_{1p} - N_{2p}\ln\nu_{2p} - N_{1m} \\ \ln\nu_{1m} - N_{2m}\ln\nu_{2m} - M_1\ln M_1 - M_2\ln M_2 \\ + N_{1p}\ln N_{1p} + N_{2p}\ln N_{2p} + N_{1m}\ln N_{1m} \\ + N_{2m}\ln N_{2m} + (M_1 - N_{1m} - N_{1p}) \\ \ln(M_1 - N_{1m} - N_{1p}) + (M_2 - N_{2m} - N_{2p}) \\ \ln(M_2 - N_{2m} - N_{2p}) \end{bmatrix} \quad (35)$$

For a binary mixture at equilibrium,

$$\left(\frac{\partial G}{\partial N_p}\right)_{N_m} = \mu_p \quad \text{and} \quad \left(\frac{\partial G}{\partial N_m}\right)_{N_p} = \mu_m \quad (36)$$

where μ_p and μ_m are the chemical potential of p- and m-xylene. Also,

$$N = N_{1m} + N_{2m} + N_{1p} + N_{2p}; \quad N_p = N_{1p} + N_{2p}; \quad N_m = N_{1m} + N_{2m} \quad (37)$$

Converting into a molar basis, Eq. 36 can be rewritten as

$$\mu_p = \left(\frac{\partial V}{\partial N_p}\right)_{N_{1m}, N_{2m}} + RT\begin{pmatrix} \ln\Lambda^3 - \frac{\partial N_{1p}}{\partial N_p}\ln\nu_{1p} - \frac{\partial N_{2p}}{\partial N_p}\ln\nu_{2p} + \frac{\partial N_{1p}}{\partial N_p}\ln N_{1p} \\ + \frac{\partial N_{2p}}{\partial N_p}\ln N_{2p} - \frac{\partial N_{1p}}{\partial N_p}\ln(M_1 - N_{1m} - N_{1p}) \\ - \frac{\partial N_{2p}}{\partial N_p}\ln(M_2 - N_{2m} - N_{2p}) \end{pmatrix} \quad (38)$$

where

$$\left(\frac{\partial V}{\partial N_p}\right)_{N_{1m}, N_{2m}} = \begin{bmatrix} \frac{\partial N_{1p}}{\partial N_p}\left(\epsilon_{p1} + \frac{N_{1p}z_1\epsilon_{p1p1}}{M_1} + \frac{N_{2p}\epsilon_{p1p2}z_{12}}{M_2} \right. \\ \left. + \frac{N_{1m}\epsilon_{p1m1}z_1}{2M_1} + \frac{N_{2m}\epsilon_{m2p1}z_{12}}{M_2}\right) + \\ \frac{\partial N_{2p}}{\partial N_p}\left(\epsilon_{p2} + \frac{N_{1m}\epsilon_{m1p2}z_{12}}{M_2}\right) \end{bmatrix} \quad (39)$$

A similar expression can be written for m-xylene.

To solve the above set of equations and, thus, obtain the adsorption isotherms, we need to evaluate the partial deriva-

tives, that is, the relation between N_{ip} and N_p (as well as N_{im} and N_m). At given values of μ_p and μ_m, N_m and N_p will be known constants. Since G, the free energy, is a minimum at equilibrium, the parameters N_{im} and N_{ip} will take on values so as to optimize G under the given constraints. Thus, the relation between N_{ip} and N_p (as well as N_{im} and N_m) can be obtained by equating the partial derivative of G with respect to N_{ip} (or N_{im}) to zero

$$0 = \left(\frac{\partial V}{\partial N_{1p}}\right)_{N_p, N_{1m}, N_{2m}} - RT\left[\ln\frac{\nu_{1p}}{\nu_{2p}} + \ln\left(\frac{N_{2p}}{N_{1p}}\frac{M_1 - N_{1m} - N_{1p}}{M_2 - N_{2m} - N_{2p}}\right)\right] \quad (40)$$

where

$$\left(\frac{\partial V}{\partial N_{1p}}\right)_{N_p, N_{1m}, N_{2m}} = \left[\begin{array}{l} \epsilon_{p1} - \epsilon_{p2} + \dfrac{\epsilon_{p1p1}N_{1p}z_1}{M_1} + \dfrac{\epsilon_{p1p2}z_{12}}{M_2}(N_{2p} - N_{1p}) \\ + \dfrac{\epsilon_{p1m1}N_{1m}z_m}{2M_1} - \dfrac{\epsilon_{m1p2}N_{1m}z_{12}}{M_2} + \dfrac{\epsilon_{m2p1}N_{2m}z_{12}}{M_2} \end{array}\right] \quad (41)$$

A corresponding set of equations can be expressed for m-xylene. The set of equations can be solved to obtain the adsorption isotherm. The single component energy and volume parameters of the model are listed here in Tables 1 and 2. The cross-component interaction terms are listed in Table 3. In the next section we will present the results from this model and compare them qualitatively with experimental data.

Using the parameters for *p*- and *m*-xylene in ORTHO silicalite, we find that m-xylene does not adsorb up to pressures of five atmospheres; at fives atmospheres, N_m is in the order of 10^{-5} molecules per unit cell. Hence, for this case, the set of equations reduces to those derived in an earlier study for single component p-xylene adsorption in ORTHO silicalite.

$\mu_m = \mu_p$: *equimolar mixture*

For the case of PARA silicalite exposed to a binary mixture of *p*- and *m*-xylene, we find more interesting scenarios. The set of equations is also more complex to solve, and we used an iterative algorithm. We first analyze the case of PARA silicalite exposed to an equimolar mixture of *p*- and *m*-xylene, that is, $\mu_m = \mu_p$. As a first approximation, Eqs. 40 and 41, and, subsequently, Eqs. 38 and 39, can be solved by neglecting the presence of any adsorbed m-xylene. This is same as Eq. 27. Thus, the adsorption isotherm for p-xylene is obtained *neglecting* the presence of m-xylene. At a given value of μ_p, we can now calculate the relation between N_{im} and N_m (substituting N_{1p} and N_{2p} calculated at that μ_p). When PARA silicalite is exposed to an equimolar binary mixture of p- and m-xylene, we find that m-xylene occupies the intersection sites with greater ease than it occupies the cross channel sites. Equations for *m*-xylene similar to Eqs. 38 and 39 can now be solved and, thus, we can obtain the adsorption isotherm for *m*-xylene when PARA silicalite is exposed to an equimolar binary mixture of *p*- and *m*-xylene. Very little *m*-xylene is adsorbed. For a second iteration, appropriate values of N_{1m} and N_{2m} can be substituted in Eqs. 40 and 41 and the entire set of equations can be solved all over again. However, the results change very little.

The adsorption isotherm for PARA silicalite exposed to an equimolar binary mixture of *p*- and *m*-xylene is shown in Figure 14. With increasing pressure, the gradual occupation of the two type of sites by *p*- and *m*-xylene are shown here. The adsorption isotherm of *p*-xylene from an equimolar *p*- and *m*-xylene mixture is almost the same as when PARA silicalite is exposed to pure *p*-xylene. The amount of *m*-xylene adsorbed is still rather small. However, in the presence of *p*-xylene, *m*-xylene adsorbs with greater relative ease than as a pure component—similar to the results of Karsli et al. (although this is not clear from the figure). At a pressure of 0.5 atmospheres, 0.01 m-xylene molecules per unit cell have adsorbed (which is five times greater than 0.002 *m*-xylene molecules that adsorb at five atmospheres when PARA silicalite is exposed to pure *m*-xylene).

The lattice model shows that more than 99% *p*-selectivity is observed when PARA silicalite is exposed to an equimolar binary mixture of *p*- and *m*-xylene. This compares reasonably with simulations of the same system (Mohanty et al., 1999), which result in about 95% *p*-selectivity. When PARA silicalite is exposed to a binary mixture with a higher concentration of *p*-xylene than *m*-xylene, we would expect that even less *m*-xylene would adsorb. However, when PARA silicalite

Table 3. Parameters for the Lattice Model for m-xylene Adsorbing in ORTHO and PARA Silicalite from Atomistic Calculations

	ORTHO Silicalite (303 K)	PARA Silicalite (303 K)
ϵ_{p1m1}	−1.5 kJ/mol	−1 kJ/mol
ϵ_{m1p2}	−15 kJ/mol	−17 kJ/mol
ϵ_{m2p1}	−11 kJ/mol	−12 kJ/mol

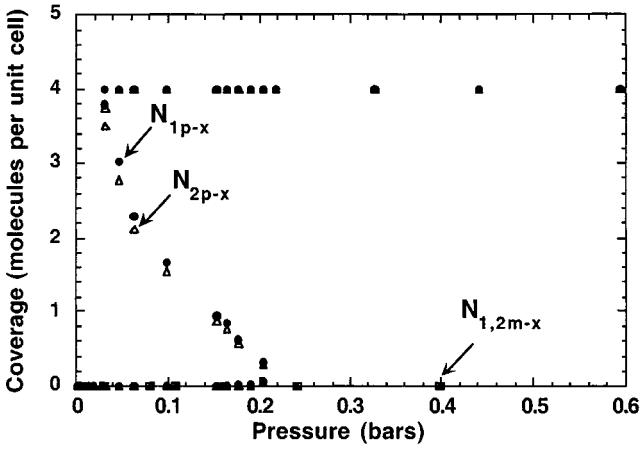

Figure 14. Adsorption isotherm for PARA silicalite exposed to an equimolar binary mixture of *p*- and *m*-xylene.

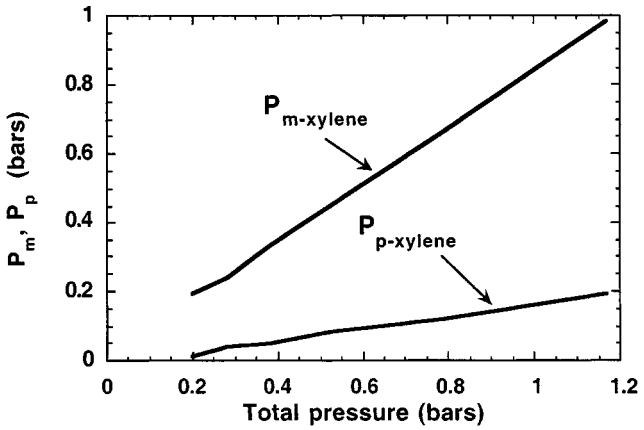

Figure 15. Partial pressures of the components relative to the total pressure.

is exposed to a binary mixture with a smaller concentration of *p*-xylene than *m*-xylene, we might expect higher amounts of *m*-xylene adsorption. Such a scenario will be analyzed next.

$\mu_m > \mu_p$: *higher concentration of m-xylene*

Similar calculations can be performed for other combinations of chemical potentials. We consider a specific case where the chemical potential of *m*-xylene is half that of *p*-xylene ($\mu_m = 0.5 \times \mu_p$) when μ_p is in the range of -120 to -60 kJ/mol, that is, the driving force of *m*-xylene is greater than that of *p*-xylene. Figure 15 shows the partial pressures of the components relative to the total pressure. We use the lattice model to calculate the adsorption isotherms of *p*- and *m*-xylene when PARA silicalite is exposed to a mixture of the components. Figure 16 plots the isotherms of *p*- and *m*-xylene adsorbing in the intersections and cross-channel sites. *p*-xylene adsorbs almost with equal ease in both types of sites, while *m*-xylene seems to adsorb more easily in the intersections. Further, *p*-xylene still adsorbs more easily than *m*-xylene. The amount of *m*-xylene adsorbed increases initially with increasing pressure (primarily at the intersection sites). However, as the partial pressure of *p*-xylene increases with increasing total pressure (Figure 15), p-xylene forces *m*-xylene out of the pore spaces. Thus, the *m*-xylene adsorption isotherm goes through a maximum. At higher pressures, where the partial pressure of *p*-xylene is significant (although much smaller than the partial pressure of *m*-xylene), the amount of m-xylene adsorbed is small (~ 0.02 molecules per unit cell).

Yet, under these conditions, *m*-xylene adsorbs more easily than from its single component state. At a total pressure of 0.3 bar (partial pressure of *m*-xylene being 0.23 bars under these conditions), the coverage of m-xylene is as high as 0.28 molecules per unit cell of PARA silicalite—a much higher coverage than any observations from single component *m*-xylene adsorption. On the other hand, comparing with a single component *p*-xylene adsorption with mixtures of various composition, *p*-xylene needs higher pressures to adsorb with increasing *m*-xylene composition. Energetically, this is because attractive interactions between *m*- and *p*-xylene is not as strong as between *p*-xylene molecules. Entropically, also a mixture of *p*- and *m*-xylene will be more favorable. Clearly then, cross component interactions has eased *m*-xylene adsorption.

Phase transition of the sorbate mixture

In Figure 14 we see very negligible *m*-xylene adsorption when PARA is exposed to an equimolar mixture of *p*- and *m*-xylene. There is no significant change in the two-phase domain from what was observed for single component *p*-xylene adsorption in PARA silicalite. Figure 16 clearly shows a metastable region in the *p*- and *m*-xylene adsorption isotherms. Further, under these conditions, a significant amount of *m*-xylene adsorbs into the pore space. Thus, we might expect a significant change in the two-phase domain from single component *p*-xylene adsorption. Figure 17 compares the two-phase region when the sorbate is pure *p*-xylene with the case of the sorbate being a *p*-/*m*-xylene mixture under the conditions shown in Figure 15. We notice that the

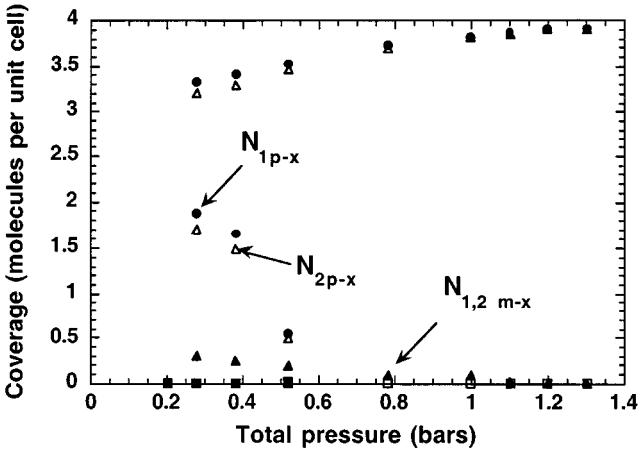

Figure 16. Adsorption isotherm for PARA silicalite exposed to a nonequilimolar binary mixture of *p*- and *m*-xylene.

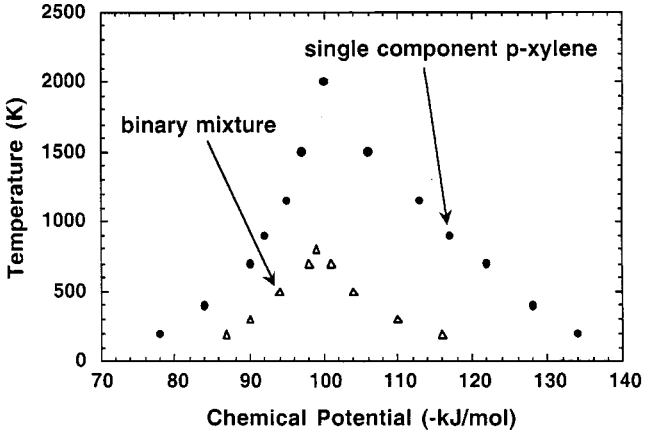

Figure 17. Comparison of the two-phase region when the sorbate is pure *p*-xylene and when the sorbate is a *p*-/*m*-xylene mixture.

two-phase region has shrunk. The critical temperature is also smaller at about 800 K. These are primarily owing to weaker sorbate-sorbate interactions in the presence of *m*-xylene.

Approximations in the Model

Let us review the approximations of this model. We have assumed the Bragg Williams approximation for the two-site model which assumes a random distribution of molecules within each type of site as the basis for calculation of configuration degeneracy and neighboring sorbate interaction energy. In a real case, however, a new sorbate molecule will have a higher probability of occupying a site of the same type, but in the neighborhood of an already sorbed molecule owing to stronger attractive sorbate-sorbate interactions. In such a case, this system of silicalite with its sorbed molecules will have a more attractive interaction energy than predicted by the Bragg-Williams approximation. Thus, the linear part of Eq. 27 will have a larger absolute slope. From Figure 9 and Eq. 27, then, it is clear that such a real system will have a larger range in μ and T where two phases (multiple roots) co-exist than predicted by the Bragg-Williams approximation. Thus, the Bragg-Williams approximation is a conservative one and, clearly, if it predicts a two-phase region, the real system certainly ought to manifest one.

We have neglected partial charges in the sorbate molecules and in the zeolite, thus dropping long-range electrostatic terms. If these are included, depending on the strengths and densities of the partial charges, we may not be able to develop the model in the manner elucidated thus far. Interactions with non-nearest neighbors may become important. Further, it may affect the onset of phase transition (Goldenfeld, 1995). However, we have observed by comparing results from an earlier work (Mohanty et al., 1999) with those of Snurr et al. (1993) and Talu et al. (1989) that neglecting partial charges does not affect the results qualitatively. It is possible that our assumption of a rigid lattice structure results in the model not appropriately capturing the effect of temperature. A rigid lattice not only influences the volume accessible for sorption, it also affects the interaction energies and, thus, the free energies defined in Eq. 4. Accounting for a flexible lattice might also change the two-phase region for the sorbate shown in Figures 7 and 11. Despite these approximations, however, the model predictions concur qualitatively with experimental results.

Conclusions

We have used a lattice model to study analytically adsorption of *p*-xylene in silicalite. This model predicts adsorption isotherms of *p*-xylene in ORTHO and PARA silicalite that qualitatively concur with experimental results. In ORTHO we do not see any sorbate phase transition at normal temperatures. However, we observe phase transition and a distinct possibility of hysteresis for *p*-xylene adsorbing in PARA silicalite. This conforms with the studies of Richards and Rees where they observe hysteresis at higher coverages. This study shows that sorbate-phase transition is a phenomenon distinct from the sorbent-phase transition observed by Koningsveld et al. (1989). The most important component for a phase transition is attractive sorbate-sorbate interactions. Based on earlier studies and this work, we conclude that in the case of p-xylene adsorbing in silicalite, the sorbent-and sorbate-phase transitions are strongly coupled. A similar study for binary mixture adsorption showed that cross component interactions strongly influence the adsorption isotherms. The two-phase region was influenced also; weaker net sorbate-sorbate interactions in the mixture (compared to single component p-xylene) caused the two phase region to shrink.

Acknowledgments

We are grateful to Drs. Ruth Ann Doyle, Jeff Miller, and Dickson Ozokwelu from Amoco chemicals for the discussions, their suggestions, and comments. The potential energy maps of xylenes in PARA silicalite were generated by Daniel Dittmer, and we are grateful to him for the same. We acknowledge support from Amoco Chemicals, Minnesota Supercomputing Institute, and the Center for Interfacial Engineering, University of Minnesota.

Literature Cited

Broughton, D. B., R. W. Neuzil, J. M. Pharis, and C. S. Brearley, "The Parex Process for Recovering Paraxylene," *Chem. Eng. Prog.*, **66**, 70 (1970).

Fyfe, C. A., G. J. Kennedy, C. T. DeSchutter, and G. T. Kokotailo, "Sorbate-Induced Structural Changes in ZSM-5 (Silicalite)," *J. Chem. Soc., Chem. Commun.*, 541 (1984).

Fyfe, C. A., H. Strobl, G. T. Kokotailo, G. J. Kennedy, and G. E. Barlow, "Ultra-High-Resolution ^{29}Si Solid-State MAS NMR Investigation of Sorbate and Temperature-Induced Changes in the Lattice Structure of Zeolite ZSM-5," *J. Amer. Chem. Soc.*, **110**, 3373 (1988).

Fyfe, C. A., Y. Feng, H. Grondey, and G. T. Kokotailo, "Characterization of a High-Loaded Intercalate of *p*-Xylene with a Highly Silecious Form of ZSM-5 by High Resolution ^{29}Si Solid-State NMR Spectroscopy," *J. Chem. Soc., Chem. Commun.*, 1224 (1990).

Goldenfeld, N., *Lectures on Phase Transitions and the Renormalization Group*, Addison−Wesley Pub. (1995).

Grauert, B., and K. Fiedler, "Monte Carlo Calculations: Thermodynamic Functions in Zeolites: II. Adsorption of Benzene on Silicalite," *Adsorp. Sci. Technol.*, **5**, 191 (1989).

Guo, C.-J., O. Talu, and D. Hayhurst, "Phase Transition and Structural Heterogeneity; Benzene Adsorption on Silicalite," *AIChE J.*, **35**, 573 (1989).

Hill, T. L., *Introduction to Statistical Thermodynamics*, Dover, New York (1986).

Karsli, H. A., A. Culfaz, and M. Yücel, "Sorption Properties of Silicalite-1 of Pure Silica Form: The Influence of Sorption Kinetics of Critically Sized Micelles," *Zeolites*, **12**, 728 (1992).

Koningsveld, H. V., F. Tuinstra, H. V. Bekkum, and J. C. Jansen, "The Location of *p*-xylene in a Single Crystal of Zeolite H-ZSM-5 with a New, Sorbate Induced Orthorhombic Framework Symmetry," *Acta Cryst.*, **B45**, 423 (1989).

Lee, C.-K., A. S. T. Chiang, and F. Y. Wu, "Lattice Model for the Adsorption of Benzene in Silicalite I," *AIChE J.*, **38**, 128 (1992).

Li, J., and O. Talu, "Structural Effect on Molecular Simulations of Tight-Pore Systems," *J. Chem Soc. Faraday Trans.*, **89**, 1683 (1993).

Mohanty, S., H. T. Davis, and A. V. McCormick, "Shape Selective Adsorption in Atomistic Nanopores—A Study of Xylene Isomers in Silicalite," *Chem. Eng. Sci.*, **55**, 2779 (2000).

Nakazaki, Y., N. Goto, and T. Inui, "Simulation of Dynamic Behavior of Simple Aromatic Hydrocarbons inside Pores of a Pentasil Zeolite," *J. Catal.*, **136**, 141 (1992).

Olson, D. H., G. T. Kokotailo, S. L. Lawton, and W. M. Meier, "Crystal Structure and Structure-Related Properties of ZSM-5," *J. Phys. Chem.*, **85**, 2238 (1981).

Pope, C. G., "Sorption of Benzene, Toluene and *p*-Xylene on ZSM-5," *J. Phys. Chem.*, **88**, 6312 (1984).

Pope, C. G., "Sorption of Benzene, Toluene and *p*-Xylene on silicalite and H-ZSM-5," *J. Phys. Chem.*, **90**, 835 (1986).

Prausnitz, J. M., R. N. Lichtenthaler, and E. G. de Azevedo. "Molecular Thermodynamics of Fluid-Phase Equilibria," Prentice-Hall, Englewood Cliffs, NJ (1986).

Rappe, A. K., C. J. Casewit, K. S. Colwell, W. A. Goddard, III, and W. M. Skiff, ''UFF, a Full Periodic Table Force Field for Molecular Mechanics and Molecular Dynamics Simulations,'' *J. Amer. Chem. Soc.*, **114**, 10024 (1992).

Reischman, P. T., K. D. Schmitt, and D. H. Olson ''A Theoretical and NMR Study of *p*-Xylene Sorption into ZSM-5,'' *J. Phys. Chem.*, **92**, 5165 (1988).

Richards, R. E., and L. V. C. Rees, ''The Sorption of *p*-Xylene in ZSM-5,'' *Zeolites*, **8**, 35 (1988).

Seko, M., T. Miyake, and K. Inada, ''Economical p-xylene and Ethylbenzene Separated from Mixed Xylene,'' *Ind. Eng. Chem. Res. Dev.* **18**, 263 (1979).

Snurr, R. Q., A. T. Bell, and D. N. Theodorou, ''Prediction of Adsorption of Aromatic Hydrocarbons in Silicalite from Grand Canonical Monte Carlo Simulations with Biased Insertions,'' *J. Phys. Chem.*, **97**, 13742 (1993).

Snurr, R. Q., A. T. Bell, and D. N. Theodorou, ''A heirarchical Atomistic/Lattice Simulation Approach for the Prediction of Adsorption Thermodynamics of Benzene in Silicalite,'' *J. Phys. Chem.*, **98**, 5111 (1994).

Talu, O., C. -J. Guo, and D. T. Hayhurst, ''Heterogeneous Adsorption Equilibria with Comparable Molecule and Pore Sizes,'' *J. Phys. Chem.*, **93**, 7294 (1989).

Thamm, H., ''Calorimetric Study on the State of Aromatic Molecules Sorbed on Silicalite,'' *J. Phys. Chem.*, **91**, 8 (1987a).

Thamm, H., ''Adsorption Site Heterogeneity in Silicalite: a Calorimetric Study,'' *Zeolites*, **7**, 341 (1987b).

Vigne-Maeder, F., and H. Jobic, ''Adsorption Sites and Packing of Benzene in Silicalite,'' *Chem. Phys. Lett.* **169**, 31 (1990).

Manuscript received Oct. 21, 1999, and revision received Feb. 25, 2000.